



# Medicinal chemistry: an effect of a desolvation penalty of an amide group in the development of kinase inhibitors

Juraj Dobias<sup>1</sup> · Marek Ondruš<sup>1</sup> · Matúš Hlaváč<sup>1</sup> · Miroslav Murár<sup>1</sup> · Juraj Kóna<sup>2</sup> · Gabriela Addová<sup>3</sup> · Andrej Boháč<sup>1,4</sup> 

Received: 3 April 2018 / Accepted: 21 August 2018 / Published online: 30 August 2018  
© Institute of Chemistry, Slovak Academy of Sciences 2018

## Abstract

An analysis of VEGFR-2 conformers from the PDB allowed us to identify an unused salt bridge containing pocket (SBCP) suitably positioned over an **AAZ** ligand (PDB: 1Y6A). The SBCP consists of Lys866, Glu883 and Phe1045. The closest distance (4.5 Å) between **AAZ** and the centre of the SBCP has *para*-carbon from the **AAZ** internal phenyl ring. This is a bit longer as required for a simple substitution on **AAZ** to interact with SBCP. To investigate ligand–SBCP interaction, we extended the structure of **AAZ** by an insertion of an amide group between an oxazole and its aromatic substituent. This allowed moving the internal Ph ring of the carboxamide ligand closer to the SBCP. Promising predictions (poses and scores) were determined for such novel ligands by the Glide (Schrödinger) and the Dock (UCSF) software. Fifteen novel carboxamides **4(a–j, l–p)** were prepared and screened. Surprisingly, their enzymatic activities are much lower (IC<sub>50</sub>: 7.6–437 μM) as expected than the **AAZ** ligand (22 nM). To explain this discrepancy, we hypothesized that high solvation energy could be a main reason for the penalty that ligands have to pay by their binding to the target. Therefore, 11 additional **AAZ** analogues possessing modified or replaced amide group by less solvated substituents **4(q–r)**; **5(a–e)**, **7(a–b)**, **9**, **10** were developed. A correlation between IC<sub>50</sub> activities and calculated solvation energies clearly supported our hypothesis. The ligands possessing less solvated group (instead of the –CONH–) were more powerful VEGFR2 TK inhibitors and vice versa. This conclusion was supported also by a significance of hydrophobic enclosure descriptor in the identified QSAR models. We can conclude that the insertion of a highly solvated extension fragment (e.g. the amide group) in the ligand should be carefully considered especially when this group will act in a hydrophobic part of a protein without forming additional interaction(s). Otherwise, the desolvation penalty of an inserted group could be a limiting factor for a ligand activity.

Juraj Dobias mainly contributed also to writing of this paper.

**Electronic supplementary material** The online version of this article (<https://doi.org/10.1007/s11696-018-0576-6>) contains supplementary material, which is available to authorized users.

✉ Juraj Dobias  
jur.dobias@gmail.com  
Andrej Boháč  
andrej.bohac@uniba.sk

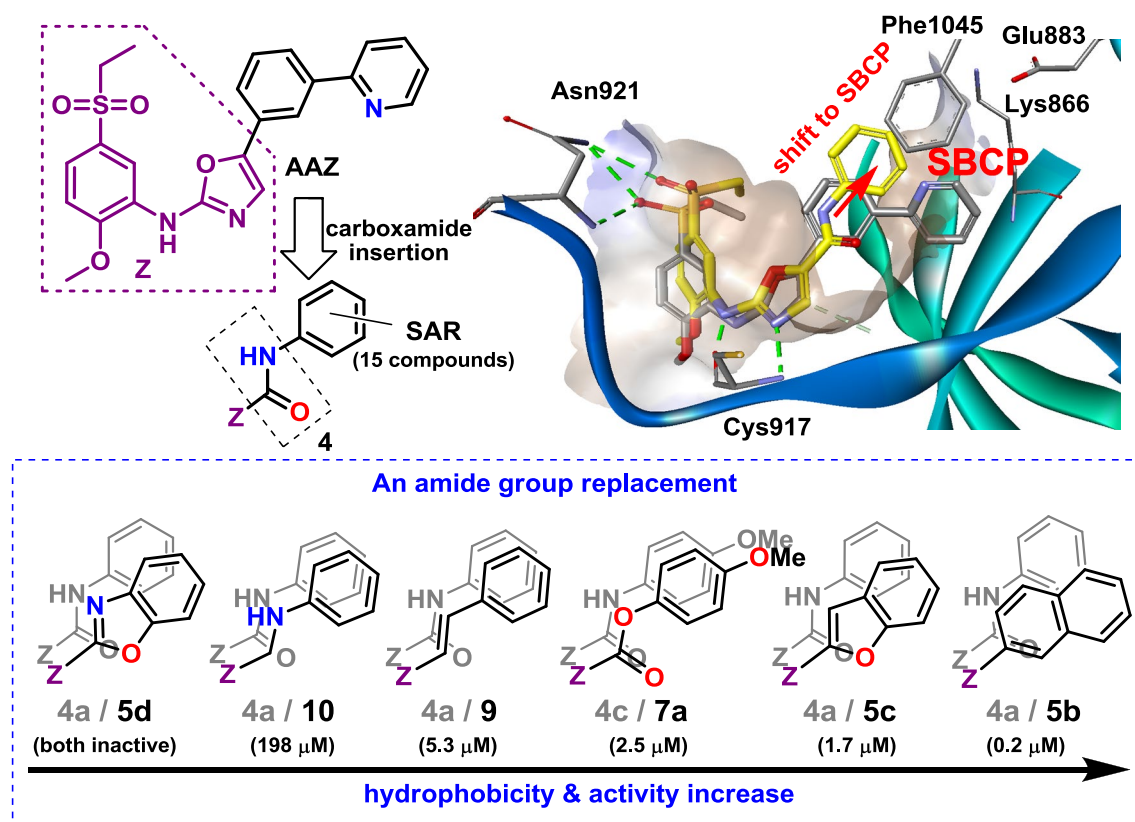
<sup>1</sup> Department of Organic Chemistry, Faculty of Natural Sciences, Comenius University in Bratislava, Mlynská dolina, Ilkovičova 6, 842 15 Bratislava, Slovakia

<sup>2</sup> Institute of Chemistry, Center for Glycomics, Slovak Academy of Sciences, Dúbravská cesta 9, 845 38 Bratislava, Slovakia

<sup>3</sup> Institute of Chemistry, Faculty of Natural Sciences, Comenius University in Bratislava, Mlynská dolina, Ilkovičova 6, 842 15 Bratislava, Slovakia

<sup>4</sup> Biomagi, Ltd., Mamateyova 26, 851 04 Bratislava, Slovakia

## Graphical abstract



**Keywords** VEGFR-2 TK SBCP pocket · Tyrosine kinase inhibitors · Amide group insertion · Energy of solvation · Desolvation penalty · 2-(Arylamino)oxazole-5-carboxamide · *N*,5-Diaryloxazol-2-amine · QSAR

## Introduction

A growing tumour requires a substantial amount of nutrition, which must be delivered by the vascular system created, e.g. by angiogenesis. Angiogenesis is a physiological process in an adult organism essential for healing of wounds or development of foetus in a woman's body (Risau 1997). In tumours, hypoxic conditions stimulate the expression of proangiogenic growth factors that are recognized by cellular receptors and cause increased division and migration of nearby vascular endothelial cells (Ferrara 2004). The most important signalling pathway that regulates angiogenesis is mediated via VEGFs and their receptors, mostly through VEGFR-2 (Finley and Popel 2012; Waltenberger et al. 1994). Small synthetic molecules that inhibit this kinase activity (by e.g. blocking of the ATP-binding site) exhibit anticancer properties (Zhang et al. 2009; Gross et al. 2015; Boyer 2002). Although more kinase drugs have appeared in recent times, the broadening of medicinal chemistry knowledge in inhibition of kinase activity is still required.

Researchers from GlaxoSmithKline (Harris et al. 2005) developed VEGFR-2 TK inhibitors based on

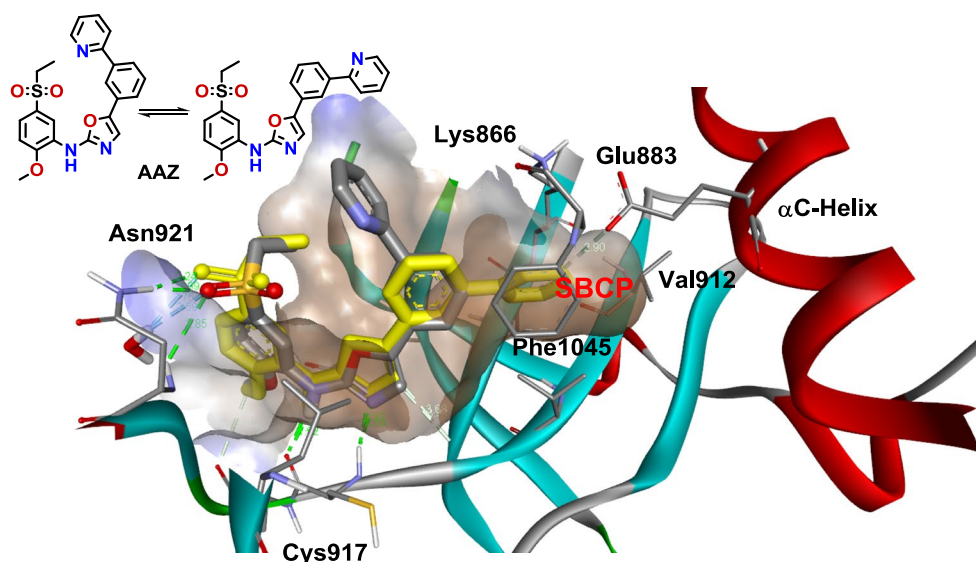
*N*,5-diaryloxazole-2-amine leading structure. They also published the crystal structure of their ligand AAZ bound to VEGFR-2 TK (PDB: 1Y6A, Fig. 1). Surprisingly, the AAZ ligand is bound there in the form of two conformers, differing in the position of pyrid-2-yl substituent. This observation inspired us in the development of several chimerical VEGFR-2 TK inhibitors (Lintnerová et al. 2014). Recently, we uncovered an unused VEGFR-2 TK binding pocket defined by a conserved salt bridge Lys866–Glu883 and Phe1045. This domain was named the salt bridge containing pocket (SBCP). We proposed that ligands could improve their VEGFR-2 binding affinity by interacting with the SBCP.

## Experimental

Synthesis of *N,N'*-diarylaminoxazole carboxamides and their analogues 4(a–p)

The amide linker in novel predicted inhibitors 4(a–j,l–p) was beneficial for their synthesis. A key synthetic step, which introduces structural variability, is a simple amide

**Fig. 1** The structure of **AAZ** ligand (present in both “U” and “S” shaped conformers) in a complex with VEGFR-2 TK (PDB: **1Y6A**, the S-conformer is marked yellow). Selected amino acid residues (important for ligand interactions or from the SBCP) and secondary structure motives are depicted too. Green dashed lines represent ligand–protein hydrogen bonds. The surface of a ligand–protein interface is depicted and coloured according to its hydrophobicity (brown: the most; blue: the least hydrophobic)



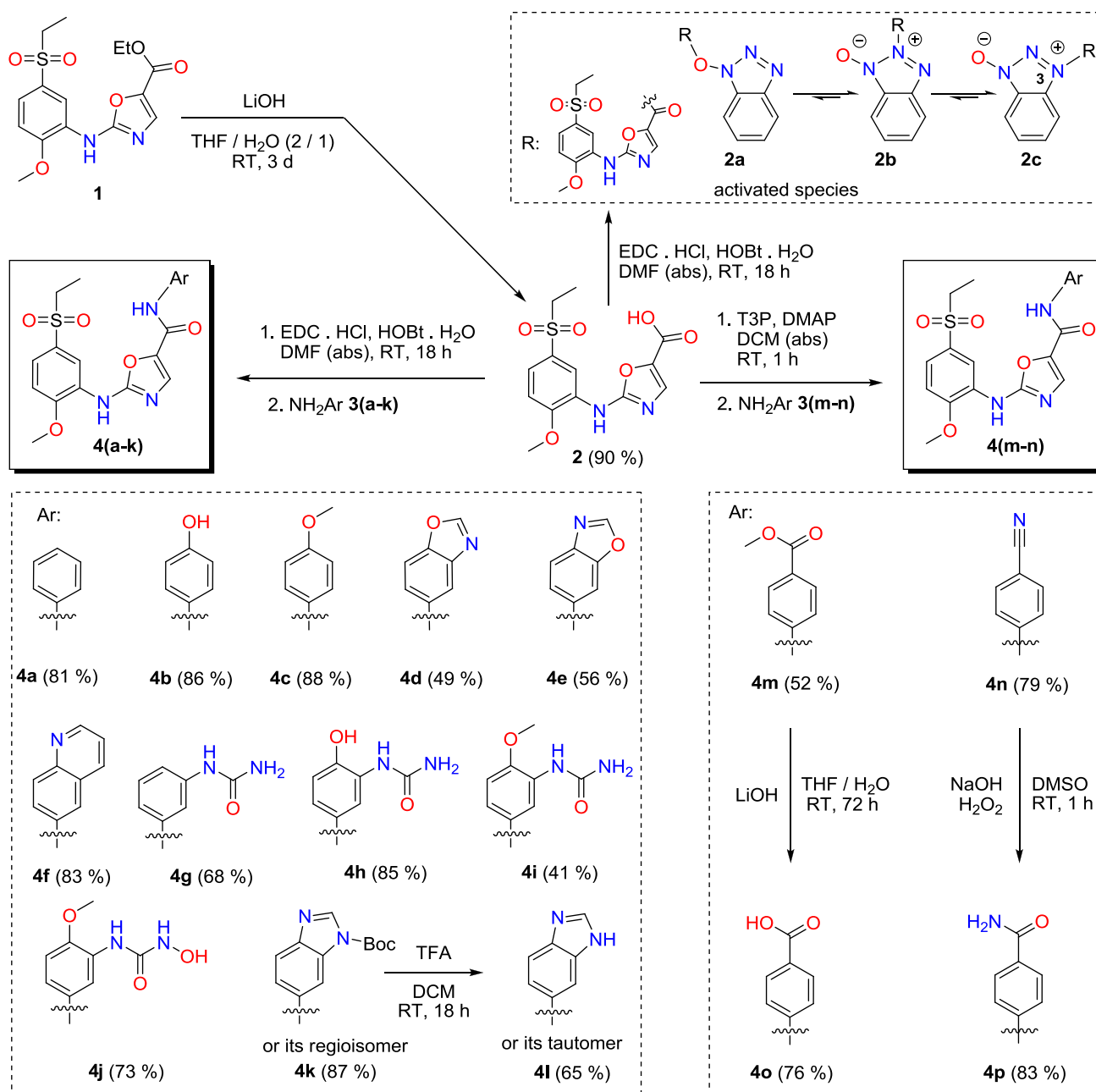
bond formation (Scheme 1), whereas for a preparation of 5-aryloxazol-2-amines **AAZ** or **5(a–c)**, it was a more difficult oxazole ring formation step (Lintnerová et al. 2015) (Scheme 4). An ester **1** was the joint precursor for the majority of the carboxamide compounds described here. The compound **1** was prepared by a method recently developed in our group (Murár et al. 2017). Most of the amides **4** were prepared via the EDC/HOBt/ArNH<sub>2</sub> procedure from an acid **2** obtained by the hydrolysis of ester **1** (Scheme 1). Some reactivity problems were encountered with less reactive *p*-EWG substituted anilines **3(m–n)**. In these cases, instead of the desired carboxamides **4(m–n)**, the activated species were isolated as a mixture of regioisomers **2(a–c)** (detected from <sup>1</sup>H-NMR). We proposed that less reactive anilines (e.g. **3m–n**) may give a time for regioisomerization of the initially formed activated ester **2a** to its less reactive forms **2(b–c)**, which further slowed down the amide bond formation for **4(m–n)** (Scheme 1). *N*(3) acylated hydroxybenzotriazole zwitterion (similar to **2c**) has already been described as the most stable isomer and its structure was solved by an X-ray crystallography (Mamos et al. 1997). The combination of AlMe<sub>3</sub> as an aniline activator with a pre-isolated mixture of the activated esters **2(a–c)** provided some amount of the carboxamide **4n** for its spectral characterization and biological assay. Later on, we found out that T3P/pyridine could be a more effective amide-coupling condition for less nucleophilic electron-poor anilines (Dunetz et al. 2011). We used DMAP instead of pyridine and obtained good yields for both carboxamides **4m** (52%) and **4n** (79%), (Scheme 1). Other carboxamides **4(l,o–p)** were prepared from their **4(k,m–n)** precursors, resp. (Scheme 1). Commercially unavailable anilines **3(d,e,h–k)** were prepared. For more details about synthesis and characterization of compounds, see the Supporting Information of this paper.

### An amide replacement: synthesis of **5(a–e)**, **7(a–b)**, **9–10**

It is known that the amide moiety is highly solvated in an aqueous environment (Makhatadze and Privalov 1993). In our case, the amide compounds **4** should reside from a water environment into the hydrophobic part of VEGFR-2 kinase upon binding. The amides **4** have to lose their solvation shell, which if not sufficiently compensated by new interactions with a host kinase causes high desolvation penalty. We thought that this might be the main mechanism responsible for the observed lower as expected VEGFR-2 TK inhibition activity of carboxamides **4(a–j,l–p)** (Scheme 6). To prove this hypothesis, we designed 11 novel ligands mimicking the above amides with modified or replaced inserted amide group and possessing less hydrophilic moieties **4(q–r)**; **5(a–e)**, **7(a–b)**, **9** and **10** (Schemes 2, 3, 4, 5).

To lower the solvation of the amide group in **4a**, we prepared its methylated analogues **4(q–r)**. The compounds were synthesized from appropriate anilines **3(q–r)** and the acid **2** by EDC/HOBt reagents (Scheme 2). The acid **2** was also utilized in the synthesis of more hydrophobic ester and carbothioate **7(a–b)**. In this case, we decided to use 4-methoxy substituted phenol **6a** and thiophenol **6b** to increase their nucleophilicity needed during esterification and stability of the targeted products **7a** and **7b**. Although previously used EDC/HOBt conditions failed, the compounds **7(a–b)** were prepared via in situ formed carboxylic chloride **2d** (Scheme 2).

To maintain higher lipophilicity and also to retain the partial double bond character of the amide bond in **4a**, an alkene **9** (Scheme 3) was prepared by the Wittig reaction from **8** in 65% yield. The aldehyde **8** was available from the ester **1** after its reduction to an alcohol and subsequent partial

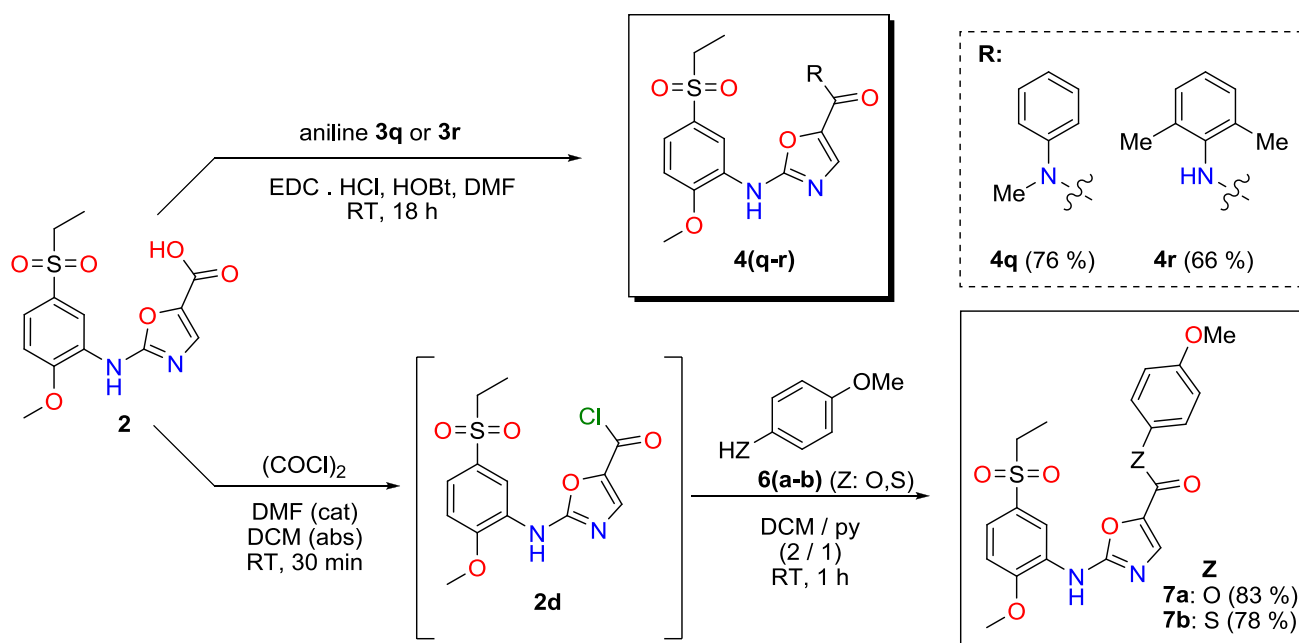


**Scheme 1** The synthesis of *N,N'*-diaryl-2-aminooxazole carboxamides **4(a-p)**

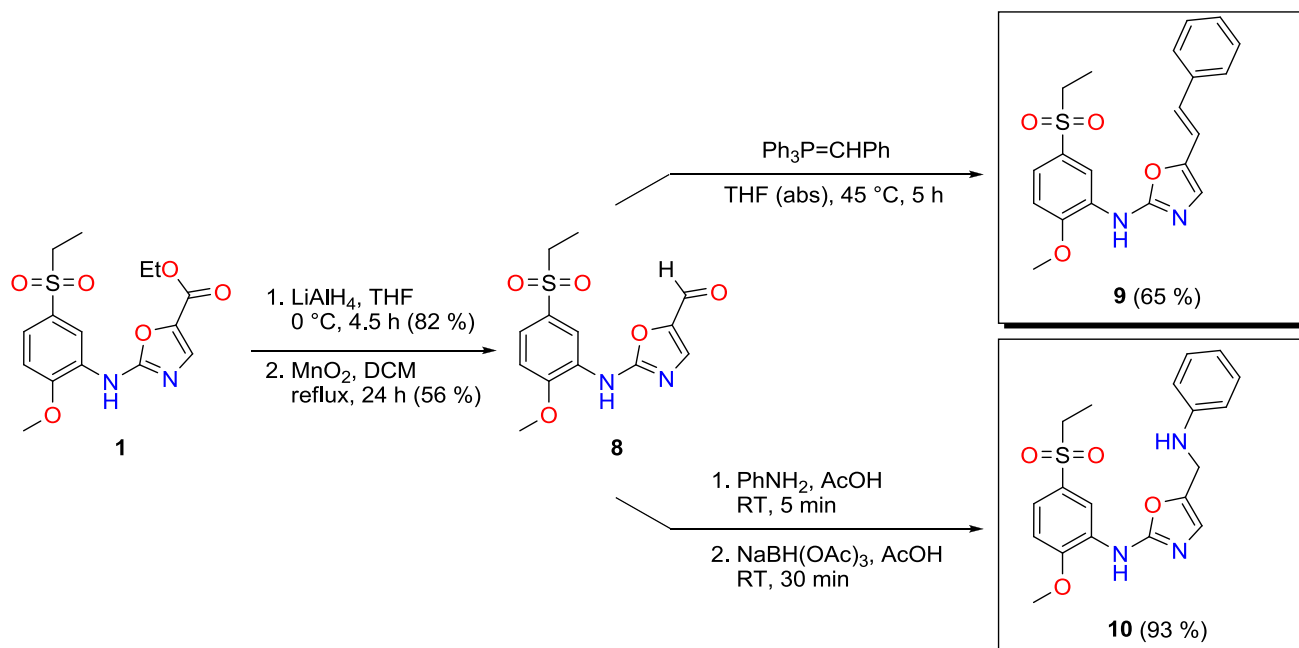
oxidation (Scheme 3) (Murár et al. 2017). An amine **10** was synthesized from the aldehyde **8** by a reductive amination in 93% yield. Compound **10** was designed with an aim of judging the influence of a carbonyl group from the amide of **4a** on VEGFR-2 TK inhibition activity.

AAZ (Fig. 1) has a lipophilic aryl group at C(5) position on the oxazole ring; therefore we decided to prepare also its simplified phenyl analogue **5a** as a standard for the biological screening (Scheme 4). The other 5-aryloxazole-2-amines **5(b-e)** were designed to be more lipophilic and aromatic bioisosteres to the standard carboxamide **4a** (Fig. 2,

Schemes 4, 5). A benzoxazole **5d** is the closest aromatic analogue to *N*-phenyl amide **4a**. A biological activity of **5d** should evaluate the importance of the aromatic bioisosteric replacement of the amide moiety in **4a** (Fig. 2, Scheme 5). One nitrogen less from **5d** should lead to a more lipophilic benzofurane **5c** (Fig. 2, Scheme 4). The most lipophilic analogue of **4a** is a naphthyl derivative **5b** (Fig. 2, Scheme 4). The crucial synthetic step for the preparation of 5-aryloxazole-2-amines **5(a-c)** was an oxazole ring formation step from an isothiocyanate **14** and an  $\alpha$ -azidoketone **13** as described in the literature (Harris et al. 2005). The



**Scheme 2** The synthesis of amides **4(q-r)**, ester **7a** and carbothioate **7b**



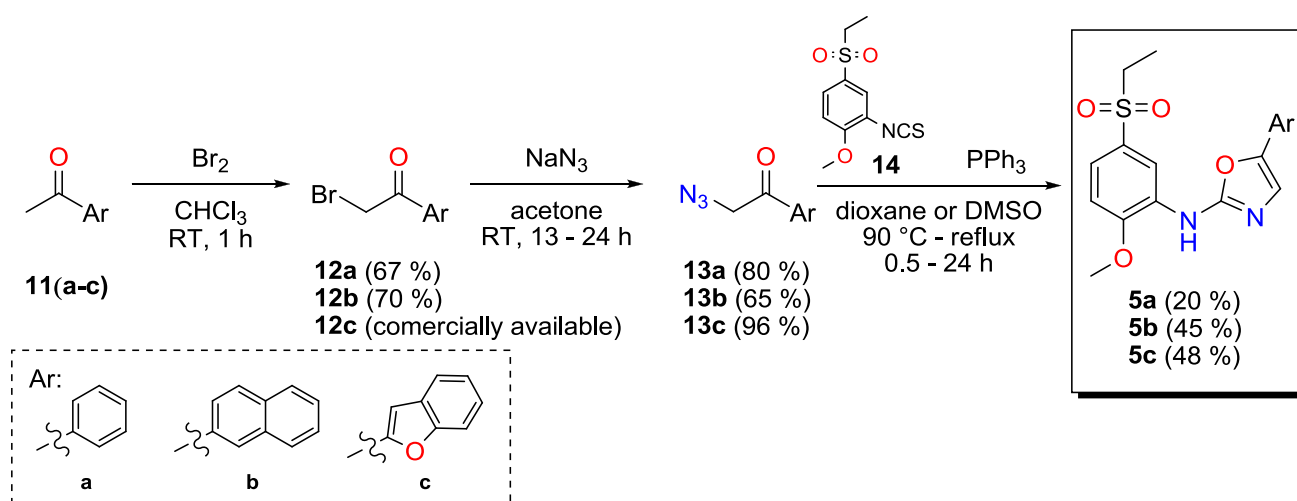
**Scheme 3** The synthesis of alkene **9** and amine **10**

preparation of  $\alpha$ -azidoketones **13** started with bromination of acetylated aromatic compounds **11** to bromoketones **12**, followed by a substitution of bromide in **12** with  $\text{NaN}_3$  to yield azidoketones **13**. Using this methodology, we synthesized compounds **5(a–c)** (Scheme 4).

Despite our intensive effort, we were not able to prepare azidoketone intermediate **13d** or its thio-analogue required

for the synthesis of benzoxazole **5d** or benzothiazole **5e**. Therefore, we selected a different synthetic pathway, which exploited the ester **1** (Scheme 5). In the literature, we noticed that benzoxazoles are frequently prepared from nitriles via imidate salts in two reaction steps. We have tried this methodology to prepare compounds **5(d–e)**. Amino thiophenol **17b** was selected at first due to its higher nucleophilicity





**Scheme 4** The preparation of 5-arylaminoxazoles **5(a-c)**

compared to aminophenol yielding **17c**. Unfortunately, a methylimidate salt **16a** caused only methylation of aminothiophenol **17b**. This alkylation reaction could have been suppressed by using a more sterically demanding *i*Pr imidate salt **16b**. However, this reaction provided only traces of the desired product **5e** and the main isolated product was the free base of imidate **16b** (Scheme 5). Alternatively, it was reported that Cu(II) ions could catalyse the formation of benzothiazole (Sun et al. 2013) and benzoxazole (Tan et al. 2012) rings from nitriles. Finally, the application of this methodology led to the synthesis of the required molecules **5(d-e)** in 59 and 79% yield, resp. (Scheme 5). For more details about syntheses and characterization of compounds, see the Supporting Information of this paper. Supporting Information contains the synthesis of 49 compounds from 35 novel substances not yet described in the literature.

## Results and discussion

### Structure design

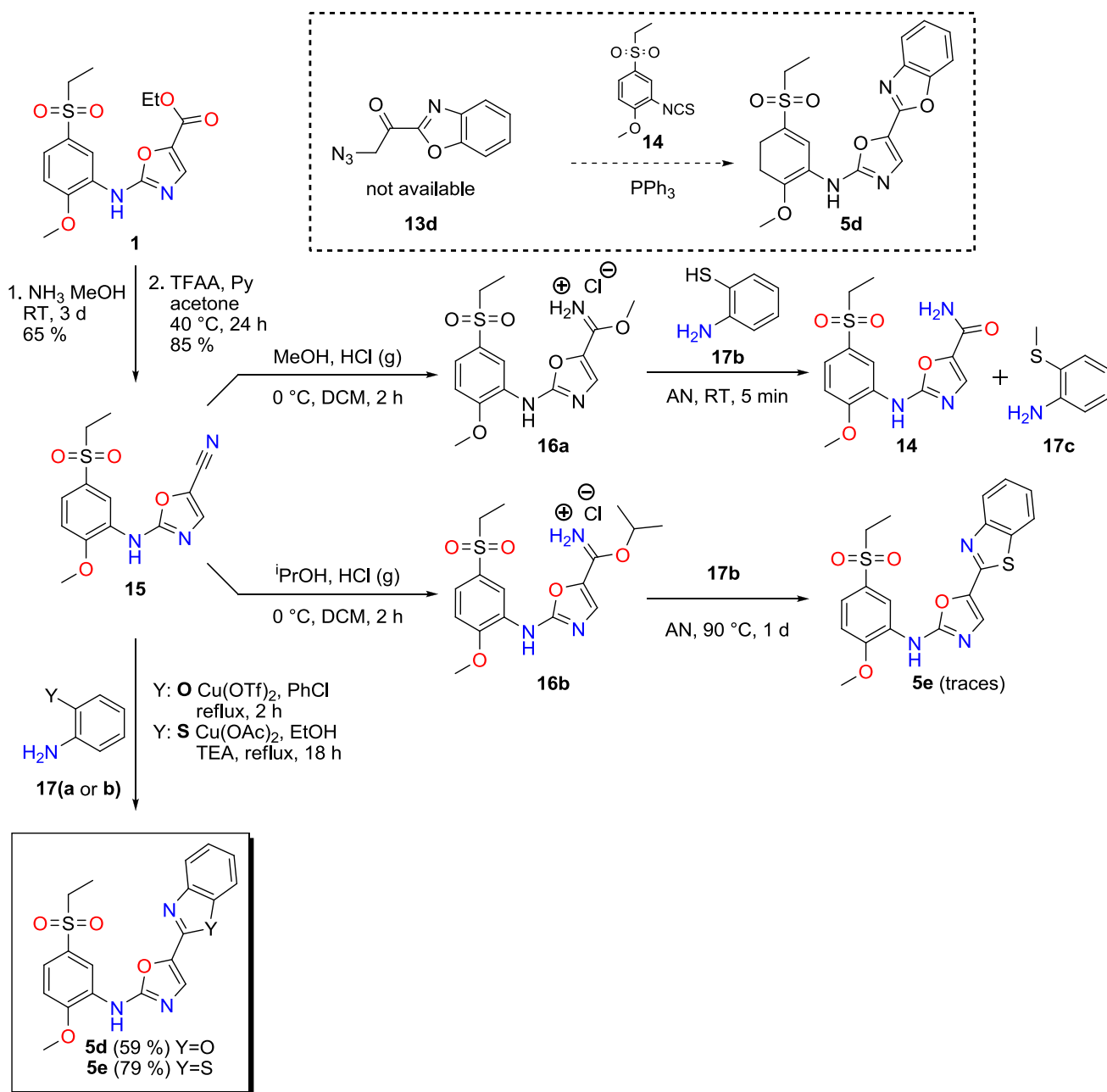
At the beginning of SBCP ligand designing, we retained the structure of **5a** (a simplified **AAZ** analogue, see Fig. 3) and tried to propose functional group(s) on its unsubstituted terminal phenyl ring. Simple substituents located there were too far to interact directly with the SBCP domain. Therefore, we decided to insert into the structure of **5a** an amide group between its oxazole and phenyl ring to get **4a** representing a new class of possible VEGFR2 TKIs (Fig. 3). This modification seemed to be promising with respect to high predicted kinase affinities for derivatives of **4** (*N*-phenyl ring was shifted closer toward the SBCP) as well as to allow

more feasible modular synthesis (a reaction between a joint carboxylic acid **2** with different anilines **3**) (Scheme 1).

The structures of 15 carboxamides **4(a-j,l-p)** were designed with consideration of the predicted ligands VEGFR-2 TK interactions, binding energies and availability of their aniline precursors **3**. Our docking studies were performed by Glide (Friesner et al. 2004, 2006; Glide and version 2016) program of the Schrödinger package and Dock of UCSF (Irwin et al. 2009) on a VEGFR-2 kinase conformer from PDB: 1Y6A (Harris et al. 2005). The predictions favoured functionalities at *m*- and/or *p*-position on **4** (Scheme 1) capable of interaction with the SBCP domain.

### Results of enzymatic assay **4(a-j,l-p)**

Fifteen prepared carboxamides **4(a-j,l-p)** were commercially screened for their VEGFR-2 TK inhibition activity (ProQuinase GmbH 2018). According to the obtained results (Scheme 6), the inserted amide group in **4** caused an unfavourable shift from a nanomolar activity of **AAZ** ( $\text{IC}_{50}$  = 46 nM) screened as a standard ( $\text{IC}_{50}$  = 22 nM from the literature (Harris et al. 2005) to the micromolar activity range for carboxamides **4(a-j,l-p)** ( $\text{IC}_{50}$  = 7.57–437  $\mu\text{M}$ ). The best compound *N'*-(benzoxazole-5-yl) amide **4e** ( $\text{IC}_{50}$  = 7570 nM) exhibited more than 32-fold increase in activity with respect to an unsubstituted *N*-phenylcarboxamide **4a** ( $\text{IC}_{50}$  = 246,000 nM). However, it is noticeable that the polar substituents present on the phenyl ring in **4** improved inhibition activities compared to **4a**, suggesting their proposed favourable interaction with the polar salt bridge from the SBCP. Relatively active compounds were also hydroxyurea **4j** ( $\text{IC}_{50}$  = 12,200 nM), benzimidazole **4l** ( $\text{IC}_{50}$  = 15,700 nM) and urea derivatives **4(i,h)** ( $\text{IC}_{50}$  = 17,800 nM, 22,100, resp.), (Scheme 6 and Fig. 4).



**Scheme 5** The alternative synthesis of benzoxazole **5d** and benzothiazole **5e** as bioisosteres of **4a**

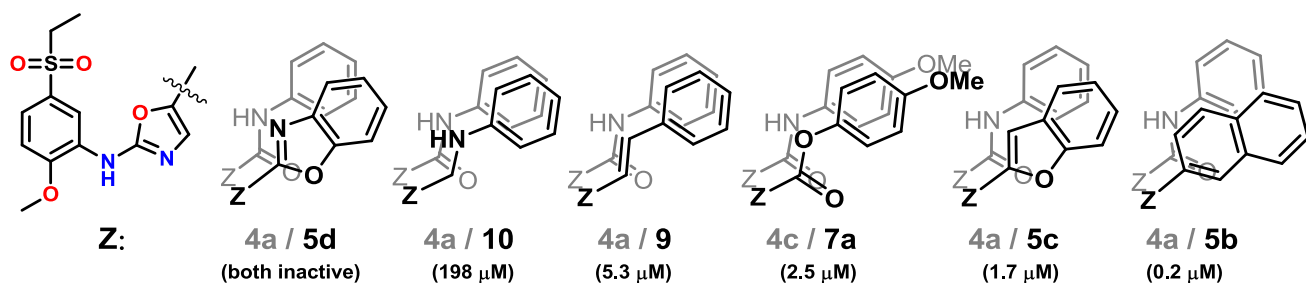


**Fig. 2** Structure superimpositions of the simplest amide **4a** with the proposed more lipophilic amide bioisosteres **5(b-d)**, **7a**, **9** and **10**

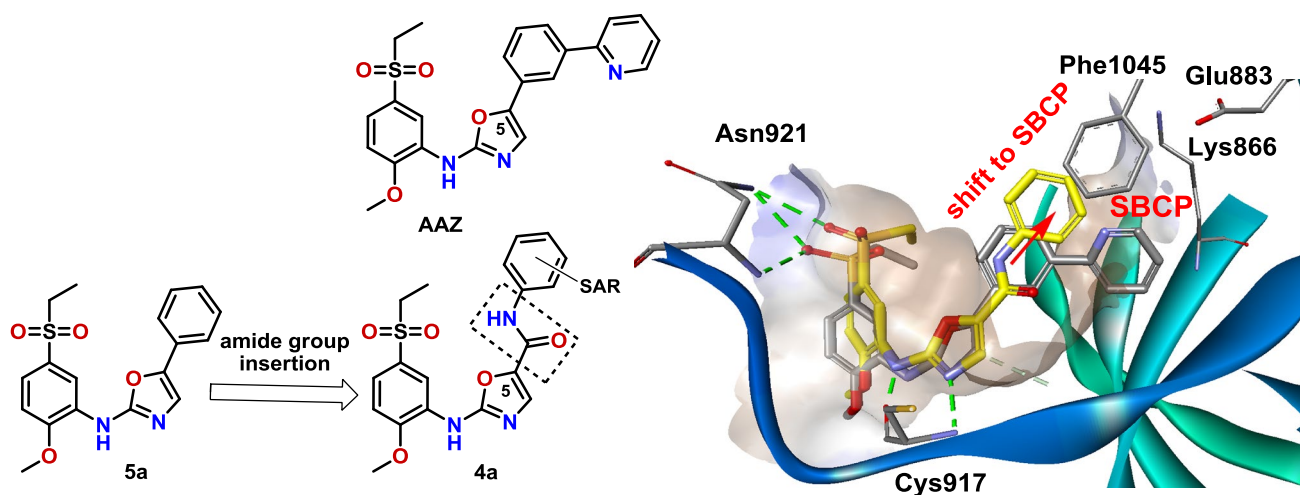


**Fig. 3** The structure of known **AAZ** VEGFR2 TK inhibitor and modification of its simplified **5a** analogue by the amide moiety insertion to form carboxamide **4a**. In the right part, the experimental binding pose of S-shaped **AAZ** conformer is depicted (grey carbon atoms)

The biological results suggested that the desired interactions with the SBCP were formed, but the activity of the carboxamides **4** was lowered probably due to the highly hydrophilic properties of the inserted amide functionality.

### Results of enzymatic assay of the carboxamide analogues **4(q–r)**; **5(a–e)**, **7(a–b)**, **9**, **10**

The other 11 compounds **4(q–r)**; **5(a–e)**, **7(a–b)**, **9** and **10** were screened for their VEGFR-2 TK inhibition activity (Reaction Biology Corp 2018). The activity for weak VEGFR2 TK inhibitors, with  $IC_{50}$  values above the concentration limit, was expressed in the form of a remaining enzymatic activity (REA) at their highest measured concentration (Table 1).

### Desolvation penalties and SAR

We performed comparisons between structures, VEGFR2 TK inhibition activities and desolvation penalties calculated between relative ligands, e.g. the pairs with or without a presence of  $-CONH-$  fragment in their structure. A correlation was observed between the less solvated ligands and the strength of their VEGFR2 TK inhibition and vice versa (see rows in Table 1).

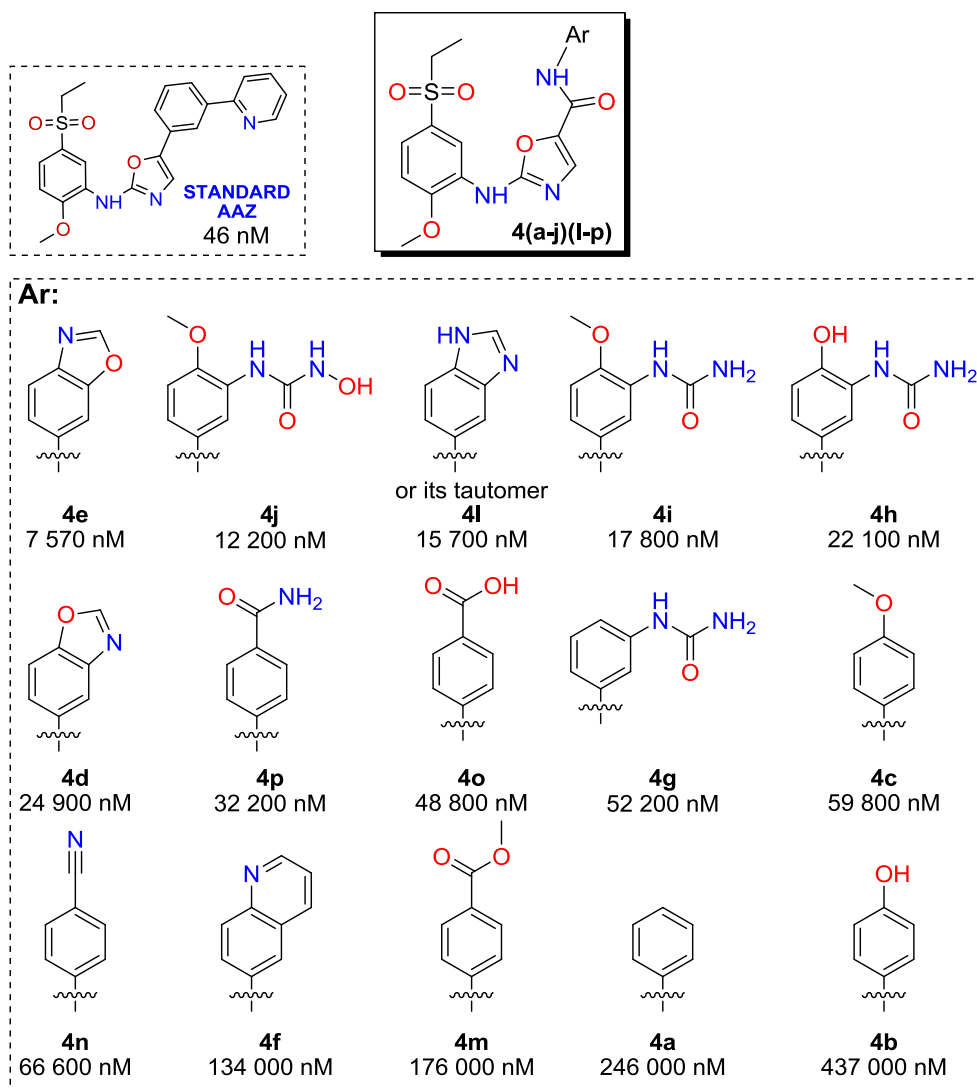
- (a) The introduction of methyl group(s) in **4r** and **4q**, which should have shielded the amide moiety from access of water, affected only a small activity improvement compared to the basic amide **4a**.

superimposed with the proposed position of the carboxamide **4a** (yellow carbon atoms) in the complex with VEGFR-2 TK (PDB: 1Y6A). The key amino acid residues together with a part of kinase hydrophobic surface and secondary structures are also depicted

- (b) A formal amide group reduction to methylamine in **10** ( $IC_{50}$  = 198,000 nM) caused an activity improvement compared to **4a**, though it was still far from the activity of the reference inhibitor **5a** (280 nM).
- (c) The bioisosteric replacements of the amide group in **4c** (REA > 80% at 500  $\mu$ M) to more lipophilic moieties (ester, or carbothioate) **7(a–b)** led to significant activity enhancement [carbothioate **7b** ( $IC_{50}$  = 9540 nM) and ester **7a** ( $IC_{50}$  = 2500 nM)]. The obtained activity of the styryl analogue **9** ( $IC_{50}$  = 5330 nM) as a more hydrophobic bioisostere of the amide **4a** clearly supported the hypothesis about the high solvation penalty of the amide group in **4** that has to be paid from their binding energy.
- (d) A replacement of *N*-phenylcarboxamide in **4a** (REA ca 80% at 500  $\mu$ M) by a relatively polar aromatic benzoxazole moiety in **5d** (REA > 75% at 100  $\mu$ M) and benzothiazole **5e** (REA > 70% at 100  $\mu$ M) gave only small activity improvement compared to **4a**. This means that a polar aromatic system at C(5) of the oxazole ring is less beneficial in our case.
- (e) The most active compounds were lipophilic aromatic bioisosteres of the *N*-Ph amide group in **4a** such as benzofuryl **5c** ( $IC_{50}$  = 1660 nM), phenyl **5a** ( $IC_{50}$  = 280 nM) and naphthyl **5b** ( $IC_{50}$  = 177 nM).

The obtained biological results revealed that VEGFR-2 TK does not tolerate highly solvated amide group at C(5) on 2-aminooxazole moiety from **4**. The hydrophobic effect between related compounds can be estimated by computation of their solvation energies in water environment. For that, we used advanced simulation of molecular





**Scheme 6** The structures of **AAZ** and 15 novel amides **4(a-j)(l-p)** sorted by their  $IC_{50}$  (VEGFR-2 TK) values

dynamics with free energy perturbation (FEP) methodology (Shivakumar et al. 2010) (for more detailed information, see Supporting Information). The calculated solvation energies are used in Table 1 to express the difference in the desolvation energy ( $\Delta\Delta G_{\text{desolv}}$ ) always between two relative compounds with ideally one structural change and determined biological activities. The VEGFR-2 TK inhibitor *N*,5-diphenylaminooxazole **5a** ( $IC_{50}$  = 280 nM,  $\Delta G_{\text{solv}}$  = − 16.0 kcal mol<sup>−1</sup>) exhibited less solvation than the almost inactive *N,N'*-diarylaminooxazole carboxamide **4a** ( $\Delta G_{\text{solv}}$  = − 19.6 kcal mol<sup>−1</sup>). Structures of the above compounds differ only by the inserted amidic group. The difference between their solvation energies should then represent the desolvation penalty  $\Delta\Delta G_{\text{desolv}} = -\Delta\Delta G_{\text{solv}} = -[\Delta G_{\text{solv}}(\mathbf{4a}) - \Delta G_{\text{solv}}(\mathbf{5a})] = -[-19.6 + 16.6] = +3.6$  kcal mol<sup>−1</sup> for **4a** caused by the presence of the amide group in the structure (Table 1, a first row). Moreover, in the case of the

carboxamide derivatives **4**, their high desolvation penalty is not compensated by additional interaction with the kinase. Therefore, the desolvation penalty of an amide group could be the main reason of the low observed biological activities in **4** compared to e.g. **5a**. See similar trends in selected pairs of compounds in the subsequent rows in Table 1. More particularly:

- (a) The computed desolvation energies (based on the unsubstituted carboxamide **4a**) were in an agreement with preserved low activity of developed amide analogues: *N*-(2,6-dimethylphenyl) amide **4r** ( $\Delta G_{\text{desolv}}$  = + 1.6 kcal mol<sup>−1</sup>), *N*-methyl amide **4q** (+ 1.4 kcal mol<sup>−1</sup>), benzoxazole **5d** (− 0.3 kcal mol<sup>−1</sup>), benzothiazole **5e** (− 0.3 kcal mol<sup>−1</sup>) and compound possessing *N*-phenylaminomethyl group **10** (− 0.7 kcal mol<sup>−1</sup>).

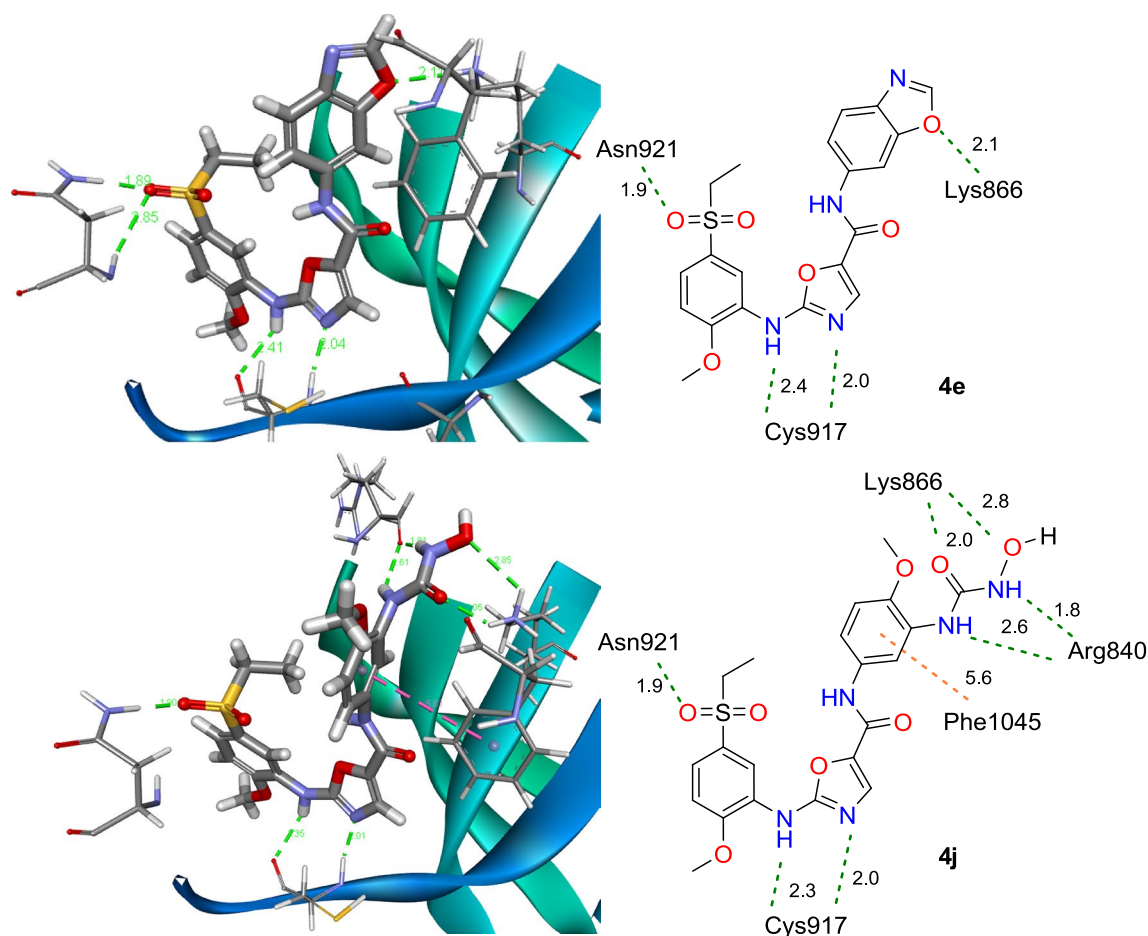


**Fig. 4** Predicted binding poses for amides **4(e-j)** in VEGFR-2 TK (PDB: 1Y6A) with their interaction diagrams on the right. Hydrogen bonds are depicted with green dashed lines and  $\pi$ - $\pi$  interactions with orange dashed lines. Each interaction has a distance specified in Å

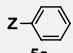
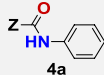
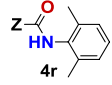
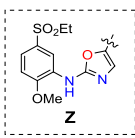
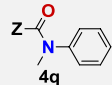
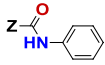
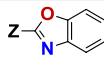
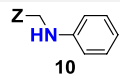
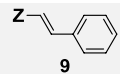
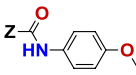
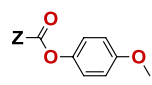
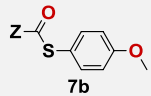
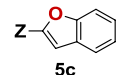
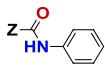
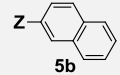
- (b) On the other hand, the negative values in  $\Delta\Delta G_{\text{desolv}}$  (Table 1) explains the kinase inhibition activity increase for styryl **9** ( $-2.9 \text{ kcal mol}^{-1}$ , 5330 nM), ester **7a** (2500 nM), benzofurane **5c** ( $-2.3 \text{ kcal mol}^{-1}$ , 1660 nM) and naphthalene **5b** ( $-2.2 \text{ kcal mol}^{-1}$ , 177 nM).
- (c) An earned difference in the desolvation energy ( $\Delta\Delta G_{\text{desolv}} = -1.0 \text{ kcal mol}^{-1}$ ) rationalizes better VEGFR-2 inhibition activity of the ester **7a** (2500 nM) compared to its carbothioate analogue **7b** (9540 nM).
- (d) The above examples show that the calculated solvation energies can explain the determined biological activity between the relative isosteric compounds: amide **4c** ( $\Delta G_{\text{solv}} = -20.6 \text{ kcal mol}^{-1}$ , almost inactive)  $\ll$  thioate **7b** ( $-18.7 \text{ kcal mol}^{-1}$ ,  $\text{IC}_{50} = 9540 \text{ nM}$ )  $<$  ester **7a** ( $-17.7 \text{ kcal mol}^{-1}$ ,  $\text{IC}_{50} = 2500 \text{ nM}$ ), sorted according to lower desolvation penalty and increased VEGFR-2 TK activity.
- (e) Moreover, less negative solvation energy of close bioisosteres means less desolvation pen-

alty and better biological activity: e.g. amide **4a** ( $\Delta G_{\text{solv}} = -19.6 \text{ kcal mol}^{-1}$ , almost inactive)  $\approx$  benzoxazole **5d** ( $\Delta G_{\text{solv}} = -19.3 \text{ kcal mol}^{-1}$ , very weakly active)  $<$  methylenamine **10** ( $\Delta G_{\text{solv}} = -18.9 \text{ kcal mol}^{-1}$ ,  $\text{IC}_{50} = 198,000 \text{ nM}$ )  $<$  styrene **9** ( $\Delta G_{\text{solv}} = -16.7 \text{ kcal mol}^{-1}$ ,  $\text{IC}_{50} = 5330 \text{ nM}$ )  $<$  benzofurane **5c** ( $\Delta G_{\text{solv}} = -17.3 \text{ kcal mol}^{-1}$ ,  $\text{IC}_{50} = 1660 \text{ nM}$ )  $<$  naphthalene **5b** ( $\Delta G_{\text{solv}} = -17.4 \text{ kcal mol}^{-1}$ ,  $\text{IC}_{50} = 177 \text{ nM}$ ) (Table 1).

## QSAR

Since predicted binding free energy ( $\Delta G_{\text{predict}}$ ) from molecular docking did not give the required accuracy (regression coefficient,  $R^2 = 0.45$ ; standard deviation,  $\text{SD} = 1.25 \text{ kcal mol}^{-1}$ , for other regression parameters see Table 2), the predictive QSAR models were composed on the experimental  $\text{IC}_{50}$  values. As a training set, 21 compounds synthesized in this and previous studies were chosen

**Table 1** A relation between selected structural changes, obtained biological activities and computed differences in desolvation energies ( $\Delta\Delta G_{\text{desolv}} = -\Delta\Delta G_{\text{solv}} = -[\Delta G_{\text{solv}}(2) - \Delta G_{\text{solv}}(1)]$ )

Structural changes	Structure 1 <sup>a</sup>	Structure 2 <sup>a</sup>	$\Delta\Delta G_{\text{desolv}}$ [kcal mol <sup>-1</sup> ]
Amide insertion	 <b>5a</b> IC <sub>50</sub> = 280 nM	 <b>4a</b> REA ca 80 % (at 500 μM)	19.6 - 16.0 = 3.6
Phenyl 2,6-dimethylation		 <b>4r</b> REA ca 70 % (at 300 μM)	21.2 - 19.6 = 1.6
N-methylation	 <b>Z</b>	 <b>4q</b> REA ca 60 % (at 300 μM)	21.0 - 19.6 = 1.4
Amide to oxazole	 <b>4a</b> REA ca 80 % (at 500 μM)	 <b>5d</b> REA > 75 % (at 100 μM)	19.3 - 19.6 = -0.3
Amide to alkylamine		 <b>10</b> IC <sub>50</sub> = 198 000 nM	18.9 - 19.6 = -0.7
Amide to alkene		 <b>9</b> IC <sub>50</sub> = 5 330 nM	16.7 - 19.6 = -2.9
Amide to ester	 <b>4c</b> REA > 80 % (at 500 μM)	 <b>7a</b> IC <sub>50</sub> = 2 500 nM	17.7 - 20.6 = -2.9
Carbothioate to ester	 <b>7b</b> IC <sub>50</sub> = 9 540 nM		17.7 - 18.7 = -1.0
Amide to “furan”		 <b>5c</b> IC <sub>50</sub> = 1 660 nM	17.3 - 19.6 = -2.3
Amide to “benzene”	 <b>4a</b> REA ca 80 % (at 500 μM)	 <b>5b</b> IC <sub>50</sub> = 177 nM	17.4 - 19.6 = -2.2

**Table 1** (continued)

Bold indicates the most important number from all three shown

The rows are ordered according to increased VEGFR2 TKI activities of the ligands

REA remaining enzymatic activity at the highest measured concentration

<sup>a</sup>VEGFR-2 TKI activities determined by RBC, USA (Reaction Biology Corp 2018)

(Lintnerová et al. 2014) (Table 3). The predictive accuracy of the models was validated on a testing set (9 structures) (Table 3 down). Using the multiple linear regression (MLR) method, the best correlated descriptor variables with experimental  $\Delta G_{\text{bind}}(\text{exp})$  were selected automatically and statistics for four QSAR models are compiled in Table 2. The most significant descriptor was shown to be a hydrophobic enclosure score ( $E_{\text{hyd\_enclosure}}$ ). Model 1 with the  $E_{\text{hyd\_enclosure}}$  descriptor provided satisfactory regression and prediction coefficients ( $R^2=0.80$  and  $Q^2=0.76$ ). By adding next descriptors (Models 2, 3 and 4), the prediction accuracy of models increased only slightly. It can be concluded that Model 2, defined as  $\Delta G_{\text{predict}} = 2.78E_{\text{hyd\_enclosure}} + 4.27\text{Glide}_{\text{Hbond}} - 3.95$ , gave the best statistics ( $Q^2=0.81$ ,  $\text{RMSD}=0.71 \text{ kcal mol}^{-1}$ ) and may be a useful predictive tool in the design of VEGFR-2 TK inhibitors with the *N*-aryl-2-aminoxazole moiety (Fig. 5). However, the predicted values of  $\Delta G_{\text{predict}}$  for new derivatives will have to be considered carefully. As it is compiled in Table 3,  $\Delta G_{\text{predict}}$  for some derivative of the testing set deviates by more than 2.0 kcal (for example, see  $\Delta G_{\text{predict}}$  for the structure of **4b**, Table 3).

## Conclusions

The primary aim of this project was the development of a novel type of VEGFR-2 TK inhibitors **4** possessing inserted amidic group that could allow reaching additional interactions with the bit more remote SBCP domain.

Several benefits were expected from the amide introduction in **4**: a/ development of a novel type of kinase inhibitors; b/ higher ligand inhibition activity based on additional interactions with the SBCP; c/ an easy preparation of diverse amide inhibitors **4** due to their modular synthesis from a joint acid **2** and different anilines **3**. To achieve these aims, we developed a series of 15 *N,N'*-diaryl-2-aminoxazole-5-carboxamides **4(a–j,l–p)**. Although their docking poses and scores in VEGFR-2 kinase (PDB: 1Y6A) indicated high possible activity, the biological assay results clearly revealed that the amide group positioned at C(5) on an oxazole in **4** was not beneficial for VEGFR-2 TK inhibition ( $\text{IC}_{50}$ : 7570–437000 nM) compared to the activity of **5a** ( $\text{IC}_{50}=280 \text{ nM}$ ) or **AAZ** ( $\text{IC}_{50}=46 \text{ nM}$ ) (Table 1 or Scheme 6, resp.). Despite the lower observed inhibition activity of **4(a–j,l–p)**, the best carboxamides indicate a favourable HB interactions with the SBCP (e.g. **4e**,  $\text{IC}_{50}=7570 \text{ nM}$ ; **4j**, 12,200 nM; **4l**, 15,700 nM; **4i**, 17,800 nM; see Scheme 6 and Fig. 4) that compensate the unfavourable effect of the present amide group. To rationalize this negative effect 11 additional compounds **4(q–r)**; **5(a–e)**; **7(a–b)**; **9** and **10** were developed and screened (see Schemes 2, 3, 4, 5 and Table 1). These compounds were designed to mask or replace the suspected polar amide group in **4** by moieties possessing similar shape, but having different hydrophilicity and aromaticity. Based on the biological activities and computation of the desolvation energies, we can conclude that the inserted amide group in **4** is not well tolerated by the VEGFR-2 kinase. This group is highly polar and well solvated by molecules of

**Table 2** Regression parameters of QSAR models built with VEGFR-2 TK inhibitors. The prediction accuracy of the models was validated with the LOO analysis

Predictive models	MLR analysis (training set)					LOO validation (training set)	
	No. desc.	$R^2$	$SD \text{ (kcal mol}^{-1}\text{)}$	$F$	$P$	$Q^2$	$\text{RMSD (kcal mol}^{-1}\text{)}$
Docking score (Glide XP)		0.45	1.25	16.4	$6.3 \times 10^{-4}$	0.36	1.29
Model 1 ( $\Delta G_{\text{predict}} = 2.54E_{\text{hyd\_enclosure}} - 6.12$ )	1	0.80	0.76	78.8	$2.3 \times 10^{-8}$	0.76	0.79
Model 2 ( $\Delta G_{\text{predict}} = 2.78E_{\text{hyd\_enclosure}} + 4.27\text{Glide}_{\text{Hbond}} - 3.95$ )	2	0.86	0.65	57.5	$8.7 \times 10^{-9}$	<b>0.81</b>	<b>0.71</b>
Model 3 ( $\Delta G_{\text{predict}} = 2.57E_{\text{hyd\_enclosure}} + 4\text{Glide}_{\text{Hbond}} - 12.85E_{\text{HOMO}} - 7.38$ )	3	0.86	0.66	38.1	$5.2 \times 10^{-8}$	0.80	0.72
Model 4 ( $\Delta G_{\text{predict}} = 2.53E_{\text{hyd\_enclosure}} + 4.86\text{Glide}_{\text{Hbond}} - 26.67E_{\text{HOMO}} + 28.4E_{\text{LUMO}} - 9.96$ )	4	0.87	0.66	28.9	$2.2 \times 10^{-7}$	0.78	0.76

$R^2$  regression coefficient,  $SD$  standard deviation for MLR analysis,  $F$   $F$  ratio,  $P$   $P$  observed significance levels for the  $T$  statistics,  $Q^2$  prediction coefficient for LOO validation test,  $\text{RMSD}$  root-mean-square deviation for LOO validation test

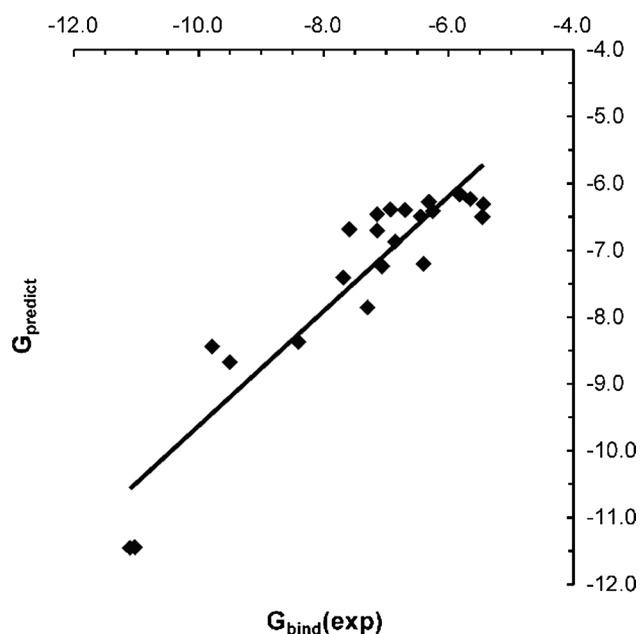
**Table 3** Experimental binding free energies [ $\Delta G_{\text{bind}}(\text{exp})$ ] calculated from  $\text{IC}_{50}$  values, docking scores (XP GlideScore) and predicted binding free energies ( $\Delta G_{\text{predict}}$ ) (Models 2 and 3) of the training and testing sets of compounds (in  $\text{kcal mol}^{-1}$ )

Compounds	$\Delta G_{\text{bind}}$ (exp)	$\Delta G_{\text{predict}}$		
		XP GlideScore	Model 2	Model 3
Training set (21 compounds)				
<b>5a</b>	− 9.50	− 9.39	− 8.67	− 8.77
<b>4j</b>	− 7.30	− 8.56	− 7.85	− 7.71
<b>5b</b>	− 9.79	− 8.52	− 8.44	− 8.61
<b>4i</b>	− 7.06	− 8.25	− 7.24	− 7.35
<b>4g</b>	− 6.40	− 8.16	− 7.20	− 7.19
<b>5c</b>	− 8.41	− 8.15	− 8.37	− 8.54
<b>9</b>	− 7.69	− 7.93	− 7.41	− 7.63
<b>4l</b>	− 7.14	− 7.64	− 6.71	− 6.73
<b>4e</b>	− 7.59	− 7.49	− 6.69	− 6.59
<b>4d</b>	− 6.86	− 7.44	− 6.87	− 6.82
<b>10</b>	− 5.46	− 7.35	− 6.50	− 6.72
<b>4h</b>	− 6.93	− 7.31	− 6.39	− 6.42
<b>4m</b>	− 5.65	− 7.30	− 6.23	− 6.13
<b>4n</b>	− 6.25	− 7.20	− 6.41	− 6.25
<b>4a</b>	− 5.44	− 7.03	− 6.31	− 6.27
<b>4o</b>	− 6.44	− 6.63	− 6.50	− 6.32
<b>4p</b>	− 6.70	− 6.54	− 6.40	− 6.27
<b>4f</b>	− 5.82	− 5.22	− 6.16	− 6.14
<b>4c</b>	− 6.32	− 5.21	− 6.27	− 6.41
<b>AAZ</b> <sup>a</sup>	− 11.02	− 7.73	− 11.45	− 11.35
<b>22SYM</b> <sup>a</sup>	− 11.10	− 10.71	− 11.45	− 11.36
Testing set (9 compounds)				
<b>33SYM</b> <sup>a</sup>	− 9.61	− 9.89	− 11.41	− 11.22
<b>23ASYM</b> <sup>a</sup>	− 10.35	− 10.44	− 11.19	− 10.98
<b>8</b> (labelled in (Lintnerová et al. 2014) <sup>a</sup>	− 9.50	− 8.39	− 8.42	− 8.47
<b>4r</b>	70% (300 μM) <sup>b</sup>	− 7.36	− 6.29	− 6.25
<b>5e</b>	70% (100 μM) <sup>b</sup>	− 7.29	− 7.80	− 7.79
<b>4q</b>	60% (300 μM) <sup>b</sup>	− 6.96	− 5.87	− 5.91
<b>5d</b>	75% (100 μM) <sup>b</sup>	− 5.02	− 7.27	− 7.40
<b>4b</b>	− 5.09	− 8.34	− 7.73	− 7.71
<b>7a</b>	− 8.15	− 7.10	− 5.87	− 5.89

<sup>a</sup>Structures and their  $\text{IC}_{50}$  values have been reported in the literature (Lintnerová et al. 2014)

<sup>b</sup>Residual enzymatic activity (REA) at specified inhibitor concentration

water. By entering the ligand into VEGFR-2 kinase, the amide group in **4** causes high desolvation penalty that importantly lowers an overall ligand binding energy. In our case, the amide group in **4** is expected to bind in a

**Fig. 5** Experimental [ $\Delta G_{\text{bind}}(\text{exp})$ ] versus predicted binding free energies ( $\Delta G_{\text{predict}}$ ) calculated from Model 2 (in  $\text{kcal mol}^{-1}$ )

hydrophobic kinase region and the above penalty cannot be compensated by additional interactions between the target and the amide group. Here, we observed an inversely proportional correlation between a ligand water solvation and its VEGFR-2 TK inhibition activity for carboxamides **4** as well as for their more lipophilic analogues **5**, **7**, **9** and **10** (Table 1). We can conclude that the substituents at C(5) on *N*-(5-(ethylsulphonyl)-2-methoxyphenyl)oxazol-2-amine (the structure **Z** in Table 1) need to be highly lipophilic to effectively inhibit VEGFR-2 TK. This idea is also supported by the significance of hydrophobic enclosure descriptor in QSAR models. The obtained models significantly improved binding energy prediction (Model 2,  $Q^2=0.81$ ) in comparison to a simple Glide XP docking score ( $Q^2=0.36$ ).

The main outcome of this paper is that an introduction of an amide group (or other highly water solvated functionality) on or into a structure of a previously active inhibitor has to be carefully considered. This is valid especially when this group is surrounded by a lipophilic region of the target and no additional compensating interactions are possible. In such a case, the calculated solvation energies between the relative compounds (e.g. amide, ester, thioate or naphthyl group) can help to estimate the ligand target activity.

**Acknowledgements** This research was supported by Biomagi, Ltd. (discovery of the SBCP pocket, an idea of an amide group insertion, Dock UCSF design of inhibitors), JD (a solvation hypothesis and calculations), VEGA 1/0670/18, VEGA 2/0064/15 (QSAR) and ITMS 26240220086 (HPLC MS). We are grateful to Mgr. Juraj Filo, PhD., for the measurement of NMR spectra.



## References

- Boyer SJ (2002) Small molecule inhibitors of KDR (VEGFR-2) kinase: an overview of structure activity relationships. *Curr Top Med Chem* 2:973–1000. <https://doi.org/10.2174/1568026023393273>
- Dunetz JR, Xiang Y, Baldwin A, Ringling J (2011) General and scalable amide bond formation with epimerization-prone substrates using T3P and pyridine. *Org Lett* 13:5048–5051. <https://doi.org/10.1021/ol201875q>
- Ferrara N (2004) Vascular endothelial growth factor as a target for anticancer therapy. *Oncologist* 9(Suppl1):2–10. <http://www.ncbi.nlm.nih.gov/pubmed/15178810>. Accessed 30 May 2017
- Finley SD, Popel AS (2012) Predicting the effects of anti-angiogenic agents targeting specific VEGF isoforms. *AAPS J* 14:500–509. <https://doi.org/10.1208/s12248-012-9363-4>
- Friesner RA, Banks JL, Murphy RB, Halgren TA, Klicic JJ, Mainz DT, Repasky MP, Knoll EH, Shelley M, Perry JK, Shaw DE, Francis P, Shenkin PS (2004) Glide: a new approach for rapid, accurate docking and scoring. 1. Method and assessment of docking accuracy. *J Med Chem* 47:1739–1749. <https://doi.org/10.1021/jm0306430>
- Friesner RA, Murphy RB, Repasky MP, Frye LL, Greenwood JR, Halgren TA, Sanschagrin PC, Mainz DT (2006) Extra precision glide: docking and scoring incorporating a model of hydrophobic enclosure for protein-ligand complexes. *J Med Chem* 49:6177–6196. <https://doi.org/10.1021/jm051256o>
- Glide, version 7.0, (2016)
- Gross S, Rahal R, Stransky N, Lengauer C, Hoeflich KP (2015) Targeting cancer with kinase inhibitors. *J Clin Invest* 125:1780–1789. <https://doi.org/10.1172/JCI76094>
- Harris PA, Cheung M, Hunter RN, Brown ML, Veal JM, Nolte RT, Wang L, Liu W, Crosby RM, Johnson JH, Epperly AH, Kumar R, Luttrell DK, Stafford JA (2005) Discovery and evaluation of 2-anilino-5-aryloxazoles as a novel class of VEGFR2 kinase inhibitors. *J Med Chem* 48:1610–1619. <https://doi.org/10.1021/jm049538w>
- Irwin JJ, Shoichet BK, Mysinger MM, Huang N, Colizzi F, Wassam P, Cao Y (2009) Automated docking screens: a feasibility study. *J Med Chem* 52:5712–5720. <https://doi.org/10.1021/jm9006966>
- Lintnerová L, García-Caballero M, Gregaň F, Melicherčík M, Quesada AR, Dobias J, Lác J, Sališová M, Boháč A (2014) A development of chimeric VEGFR2 TK inhibitor based on two ligand conformers from PDB: 1Y6A complex—Medicinal chemistry consequences of a TKs analysis. *Eur J Med Chem* 72:146–159. <https://doi.org/10.1016/j.ejmech.2013.11.023>
- Lintnerová L, Kováčiková L, Hanquet G, Boháč A (2015) Selected methodologies convenient for the synthesis of *N*,5-diaryloxazole-2-amine pharmacophore. *J Heterocycl Chem* 52:425–439. <https://doi.org/10.1002/jhet.2063>
- Makhatadze GI, Privalov PL (1993) Contribution of hydration to protein folding thermodynamics. I. The enthalpy of hydration. *J Mol Biol* 232:639–659. <https://doi.org/10.1006/jmbi.1993.1416>
- Mamos P, Papaioannou D, Kavounis C, Nastopoulos V (1997) (*S*)-3-(*O*-methyl-*N*α-triphenylmethylglutamyl)benzotriazole 1-oxide. *Acta Crystallogr Sect C Cryst Struct Commun* 53:1973–1975. <https://doi.org/10.1107/S0108270197011591>
- Murár M, Dobias J, Šramel P, Addová G, Hanquet G, Boháč A (2017) Novel CLK1 inhibitors based on *N*-aryloxazol-2-amine skeleton—a possible way to dual VEGFR2 TK/CLK ligands. *Eur J Med Chem* 126:754–761. <https://doi.org/10.1016/j.ejmech.2016.11.003>
- ProQuinase GmbH. <https://www.proquinase.com/>. Accessed 8 Mar 2018
- Reaction Biology Corp. [www.reactionbiology.com](http://www.reactionbiology.com). Accessed 8 Mar 2018
- Risau W (1997) Mechanisms of angiogenesis. *Nature* 386:671–674. <https://doi.org/10.1038/386671a0>
- Shivakumar D, Williams J, Wu Y, Damm W, Shelley J, Sherman W (2010) Prediction of absolute solvation free energies using molecular dynamics free energy perturbation and the opl force field. *J Chem Theory Comput* 6:1509–1519. <https://doi.org/10.1021/ct900587b>
- Sun Y, Jiang H, Wu W, Zeng W, Wu X (2013) Copper-catalyzed synthesis of substituted benzothiazoles via condensation of 2-aminobenzenethiols with nitriles. *Org Lett* 15:1598–1601. <https://doi.org/10.1021/ol400379z>
- Tan H, Pan CX, Xu YL, Wang HS, Pan YM (2012) Synthesis of benzoxazoles by the copper triflate catalysed reaction of nitriles and *o*-aminophenols. *J Chem Res* 36:370–373. <https://doi.org/10.3184/174751912X13360692916944>
- Waltenberger J, Claessonwelsh L, Siegbahn A, Shibuya M, Heldin C (1994) Different signal-transduction properties of Kdr and Flt1, 2 receptors for vascular endothelial growth-factor. *J Biol Chem* 269:26988–26995. <http://www.jbc.org/content/269/43/26988.long>. Accessed 8 Mar 2018
- Zhang J, Yang PL, Gray NS (2009) Targeting cancer with small molecule kinase inhibitors. *Nat Rev Cancer* 9:28–39. <https://doi.org/10.1038/nrc2559>